Eur. J. Mech. B/Fluids 18 (1999) 659–674

Characteristics of the near wake of a cylinder at low Reynolds numbers

P. Paranthoën [a,*], L.W.B. Browne [b], S. Le Masson [a,1], F. Dumouchel [a], J.C. Lecordier [a]

[a] *UMR 6614, C.N.R.S., Université de Rouen, 76821 Mont Saint Aignan cedex, France*
[b] *Department of Mechanical Engineering, University of Newcastle, NSW 2308, Australia*

(Received 26 May 1998; revised and accepted 23 October 1998)

Abstract – An experimental study has been made of the near wake of two two-dimensional bluff bodies, a circular cylinder and a flat ribbon in the regimes corresponding to the 2-D steady and 2-D periodic wake. Velocity measurements from both hot-wire and laser Doppler anemometry are compared. Detailed measurements of the velocity field in air in the near wake, in isothermal conditions, are presented. The evolutions of the mean longitudinal velocity and the rms transverse velocity fluctuation on the center line can be plotted in a universal form whatever the value of the Reynolds number. These measurements show also that the onset of the instability is related to a critical value of an interaction term characteristic of the strength of the shear layers and the shear layer spacing at the end of the recirculation zone. © Elsevier, Paris

1. Introduction

Since the early works of Bénard [1] and von Karman [2] the phenomenon of vortex shedding behind bluff bodies, at low Reynolds numbers, has attracted considerable attention. Numerous investigations have provided much detailed information on various aspects of this problem. For example, the longitudinal and lateral spacing of vortices, the time frequency of the vortex pattern with Reynolds numbers and vortex street drag have been widely studied by Kovasznay [3], Roshko [4,5], Abernathy and Kronauer [6], Bearman [7].

Important progress has been made over the last decade in explaining some particular characteristics of laminar vortex shedding found in earlier studies. Thus, for example, there is now an understanding of the existence of the discontinuities found in the Strouhal–Reynolds number dependency and the related oblique and parallel modes of vortex shedding at low Reynolds numbers, Gerich and Eckelmann [8], Van Atta and Gharib [9], Williamson [10,11], König et al. [12].

In parallel, the development of the analysis of linear and non linear stability has led to significant progress in recent years. Most of these studies have been related to the concepts of local–global absolute-convective instability, Koch [13], Triantafyllou et al. [14], Monkewitz [15], Yang and Zebib [16], Huerre and Monkewitz [17], Oertel [18] and to the use of the Landau–Stuart equation, Provansal et al. [19], Goujon-Durand et al. [20], Dusek et al. [21]. In parallel 2D or 3D numerical simulations of the Navier–Stokes equations of this flow have been carried out, Son and Hanratty [22], Persillon and Braza [23].

However as mentioned by Yang and Zebib [16] a part of these calculations is dependent on the sparse available velocity profiles of the near wake. Most of these velocity data have been obtained by means of hot-wire anemometry and are not always very accurate, Kovasznay [3], Nishioka and Sato [24]. Some results are now available obtained by LDA, Le Masson [25], Goujon-Durand et al. [20], Paranthoën et al. [26], or PIV, Gharib

* Correspondence and reprints
[1] Present address: CNET, Technopole Anticipa, 22037 Lannion cedex, France

et al. (quoted by Williamson [11]). This small amount of information concerning the near wake can be related to the experimental difficulties of carrying out measurements at low Reynolds numbers. In air, for example, flow measurements have to be made at very low velocities (lower than 0.5 m/s) in the wake of a very small dimension cylinder (diameter about 1 mm) in order to study the laminar vortex shedding. Furthermore some experimentalists have mentioned that the use of a hot-wire could perturbate the vortex shedding phenomenon itself, Kovasznay [3], Berger quoted by Mair and Maull [27].

The first motivation of this experimental investigation was to compare experimental results of the velocity field in the near wake of a circular cylinder by using both hot-wire and laser Doppler anemometry (LDA).

The second motivation was to bring some new elements to the large amount of existing, somewhat puzzling, information concerning the characteristics of the near wake behind a bluff body at low Reynolds numbers just under and above the critical Reynolds number.

2. Experimental setup

These experiments were carried out in air in the potential core of a laminar plane jet. The plane jet facility consists of a variable speed blower supplying air to a two-dimensional rectangular 10 : 1 contraction. The jet exits normally to an end plate (17 cm × 35 cm) from a slit of width $b = 1.5$ cm and span 15 cm centrally located in this plate. To minimize air turbulence, large chambers with baffles and sound absorbing material were used between the fan and the contraction. On the centerline at the nozzle exit the turbulence intensity σ_u^* is approximately 0.4%.

The vortex shedding bluff body was a smooth stainless steel $d = 1$ mm diameter tube mounted horizontally in the middle of the jet close to the exit plane. Its total length was 15 cm ($L/d > 150$). In order to avoid vibrations, the circular cylinder was damped with pieces of foam located at the ends. Further, to prevent oblique shedding, four parallel 100 μm diameter wires were located on each edge of the jet exit plane perpendicular to the cylinder. The distance between these wires was about 1 mm. This system is similar to the one used by Hammache and Gharib [28] consisting of two upstream circular cylinders positioned normal to the obstacle.

With the selected diameter, $d = 1$ mm, Reynolds numbers $Re = U_\infty d/\nu_g$ from 34 up to 75 could be obtained by varying the upstream velocity U_∞ between 0.5 m/s and 1.15 m/s. Here ν_g is the kinematic viscosity of the fluid at the temperature of the upstream flow.

About ten cases were studied: $Re - Re_c = -9.3, 4, 6, 8, 10, 12.7, 15, 20, 30$ including the two cases studied by Kovasznay [3]: $Re - Re_c = -9.3, 12.7$. The critical Reynolds number Re_c was about 43.3. Some measurements were also carried out with a flat ribbon (1 mm × 80 mm). The critical Reynolds number of the ribbon was 32.

Velocity measurements were made using successively a hot-wire anemometer and an LDA system. We used an LDA TSI system incorporating a 1.5 W Spectra Physics laser system, an integrated optical transmission unit and a light collecting system for the forward scattering mode. The optical measuring volume was $0.08 \times 0.08 \times 1.4$ mm^3 with the major axis parallel to the cylinder. The sampling rate was very low and no correction was made for sampling bias. The location of the center of the measuring volume was accurately obtained by studying the light scattered by a 20 μm wire on which the measuring volume was adjusted. The location of the wire was known by displacing it from the surface of the cylinder after electric contact.

We concurrently carried out velocity measurements by operating a 1210 T1.5 TSI probe at an overheat ratio of 1.5 using a DANTEC 55M01 constant temperature anemometer. The calibration of the hot-wire was carried out in the core of the laminar plane jet between 0.05 m/s and 1 m/s with the LDA system.

As shown in *figure 1* the origin of the coordinate system was taken at the center of the cylinder. The x axis was measured in the direction of the flow, the y axis was perpendicular to the flow and the z axis coincided

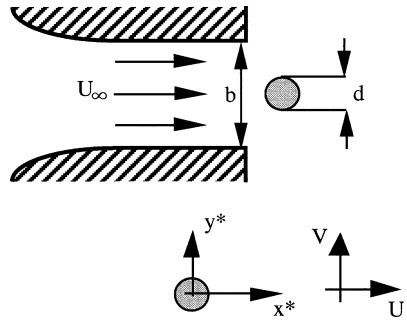

Figure 1. Experimental set-up.

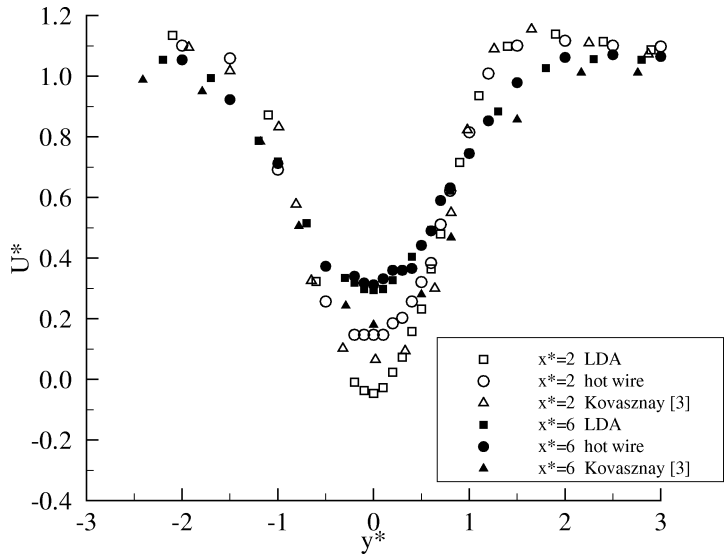

Figure 2. Mean longitudinal velocities in the cylinder wake measured by LDA and hot-wires. $Re - Re_c = -9.3,\ x^* = 2,\ x^* = 6.$

with the cylinder axis. In our study all the lengths are non-dimensionalized by the diameter d of the cylinder ($x^* = x/d,\ y^* = y/d$) and the velocities are normalized by the upstream velocity U_∞. σ_u and σ_v are the rms values of longitudinal and transverse velocity fluctuations respectively.

3. Comparisons of hot-wire and laser Doppler anemometer measurements

A systematic comparison of velocity measurements obtained by means of the hot wire and LDA systems has been made for several Reynolds numbers. In *figures 2* and *3* are some examples of this comparison for $Re = 34$ ($Re - Re_c = -9.3$, no vortex shedding) and 56 ($Re - Re_c = 12.7$, vortex shedding), the same Reynolds numbers chosen by Kovasznay [3], whose results are presented for comparison.

As shown in *figures 2* and *3* measurements made with a hot-wire at $x^* = 2$ obviously do not show the reversed flow existing in the wake bubble and lead in the shear layers to higher values of the longitudinal velocity in comparison with LDA measurements. Further downstream at $x^* = 6$ and 8 the differences between the longitudinal mean velocity U^* measured by hot-wire and LDA become less important.

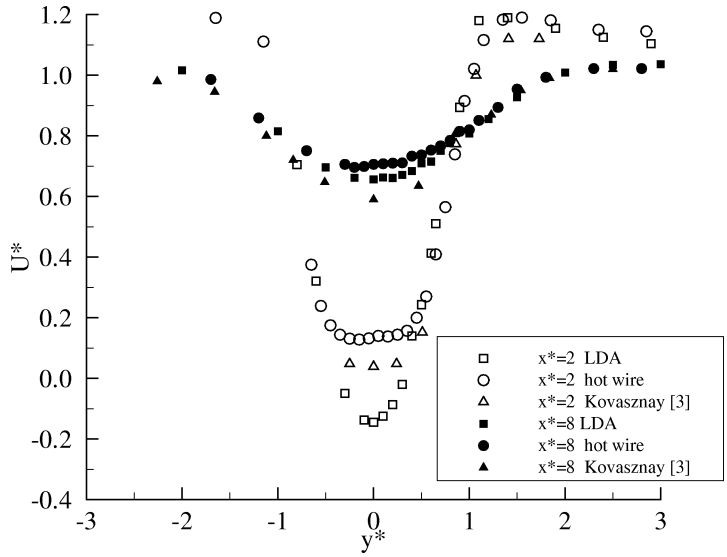

Figure 3. Mean longitudinal velocities in the cylinder wake measured by LDA and hot-wires. $Re - Re_c = 12.7,\ x^* = 2,\ x^* = 8.$

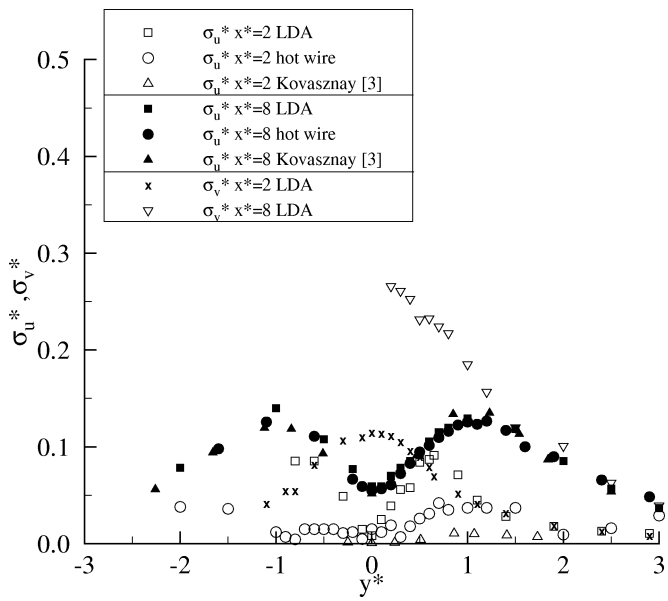

Figure 4. Comparisons between the intensities of longitudinal velocities in the cylinder wake measured by LDA and hot-wires. $Re - Re_c = 12.7$, $x^* = 2$, $x^* = 8$.

On the other hand the results presented in *figure 4* for $Re = 56$ at $x^* = 2$ show that measurements made with the hot-wire always underestimate the longitudinal velocity intensity $\sigma_u^* = \sigma_u / U_\infty$. In *figure 4* the transverse velocity intensity $\sigma_v^* = \sigma_v / U_\infty$, measured at $x^* = 2$ and 8 by LDA, is also presented for comparison. Again the differences observed between the measured values of σ_u^* with hot-wire and LDA decrease with increasing values of x^*. At $x^* = 8$ a good agreement is found between results obtained by hot-wire and LDA measurements and the measurements of Kovasznay [3].

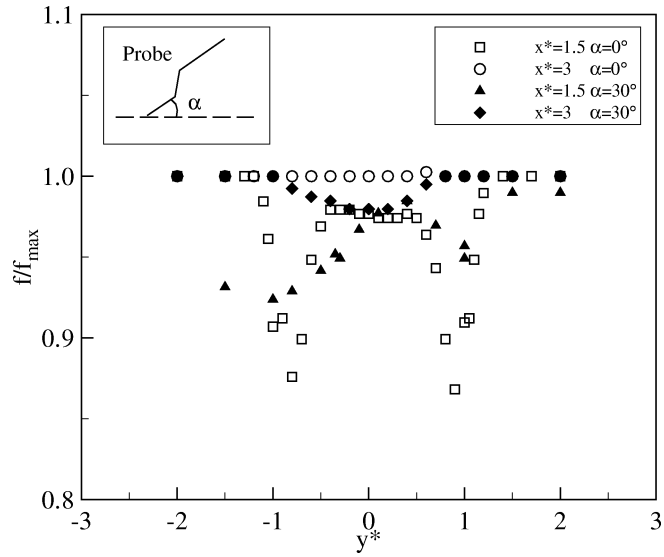

Figure 5. Influence of the hot-wire location on the vortex shedding frequency from the cylinder. $Re - Re_c = 6.7$, wire inclination angle: 0° and 30°.

The present results confirm that a conventional single hot-wire actually measures the absolute value of the velocity vector in this two-dimensional flow. In the near wake where the contribution of the instantaneous transverse velocity is never negligible in comparison with the longitudinal one, the hot-wire overestimates the mean longitudinal velocity. This happens also on the centre line where the mean velocity V^* is zero, σ_v being always much higher than σ_u. For example, at $Re - Re_c = 12.7$ the local intensity can reach 15% for u' and 60% for v' at $x^* = 6$ on the centre line. These relatively high values of the velocity intensities can also lead to heat-transfer and quadratic non-linearities, Perry [29], Bruun [30].

Furthermore the sensitivity of vortex shedding at low Reynolds numbers to the presence of a hot-wire in the near wake has been reported by Kovasznay [3] and mentioned by Berger, Mair and Maull [27]. As with Berger, we have found that the insertion of a hot-wire in the shear layer resulted in a decrease of the vortex shedding frequency. As shown in *figure 5* this effect was present for $Re = 50$ ($Re - Re_c = 6.7$) when the hot-wire was located in the near wake ($x^* = 1.5$) and disappeared for $x^* = 3$ for the horizontal probe. This effect was found to be symmetrical only when the probe axis was parallel to the upstream flow.

This phenomenon, linked to the presence of a heated hot-wire in the near wake has to be related to the experimental results of Strykowski and Sreenivasan [31] and Paranthoën and Lecordier [32]. These authors have shown that vortex shedding can be altered by the placement of a second, much smaller cylinder, in the near wake of the main cylinder. This last phenomenon brings into question the validity of hot-wire measurements made close to the cylinder just above the critical Reynolds number.

The analysis of these experimental limitations led us to prefer the LDA system for the velocity measurements in the near wake. The hot-wire was only used for measurements of the frequency and wave length at some distance from the bluff body.

4. Velocity results

In this section we present some results concerning the velocity field downstream of the circular cylinder, 1 mm diameter. Before showing these results some general characteristics of the wake are presented. These

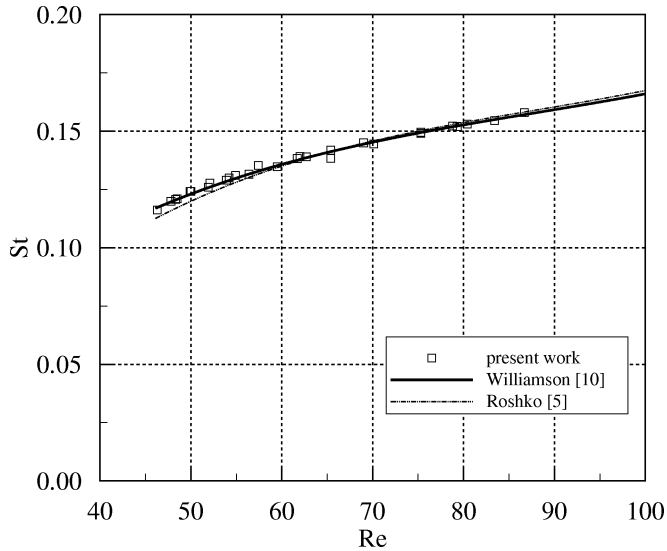

Figure 6. Strouhal number as a function of the Reynolds number.

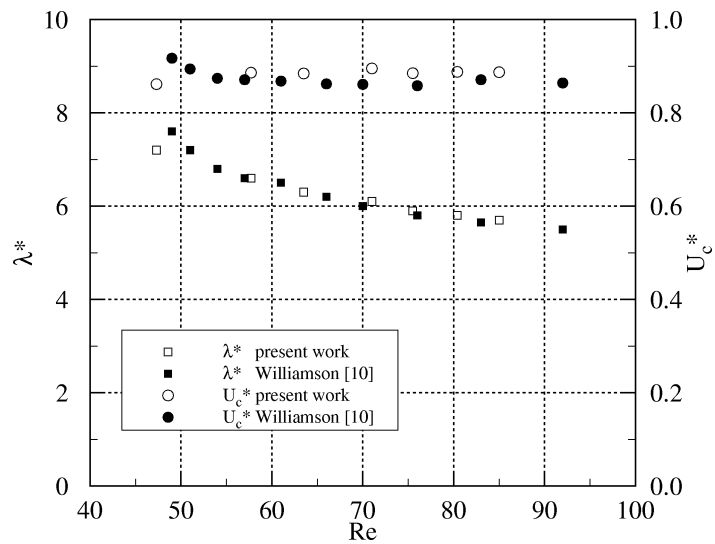

Figure 7. Wave length and convection velocity as a function of the Reynolds number.

results concern the Strouhal number $St = fd/U_\infty$, the wave length $\lambda^* = \lambda/d$ and the convection velocity U_c^* measured in the wake slightly off the centerline at $x^* = 10$. These results are presented in *figures 6* and *7* and agree reasonably well with the results of Roshko [4] and Williamson [10].

The velocity distributions were measured for nine values of the Reynolds number: $Re - Re_c = -9.3, 4, 6, 8, 10, 12.7, 15, 20, 30$ at various positions ($1 < x^* < 15$) in the wake. These profiles are shown in *figures 8* and *9* for $Re - Re_c = -9.3$ and 10 only. They are always symmetrical about the center line. They show the existence of the recirculation zone close to the cylinder and then the evolution of the velocity defect in the wake. As shown in *figure 8* a good agreement is found at $x^* = 2$ and 5 between our results and the velocity profiles calculated by Yang and Zebib [16] at the same Reynolds number.

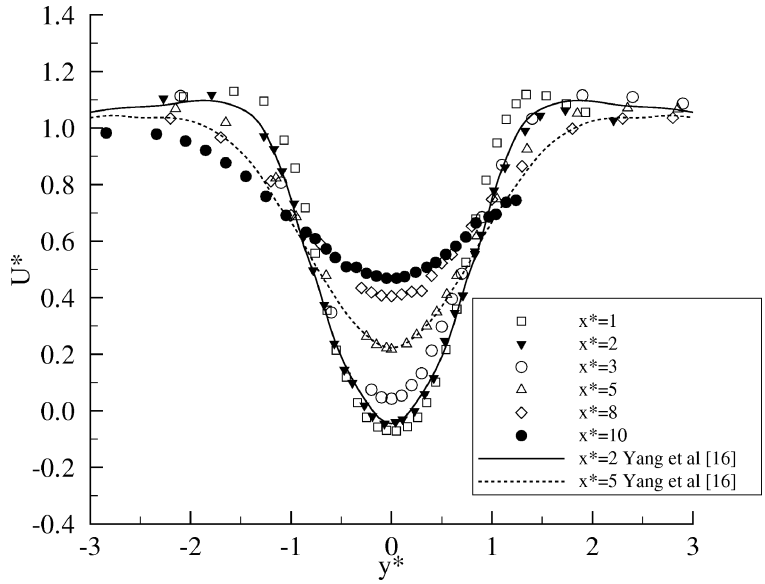

Figure 8. Mean longitudinal velocities in the cylinder wake. $Re - Re_c = -9.3,\ x^* = 1, 2, 3, 5, 8, 10$. Comparison with the results of Yang and Zebib [16].

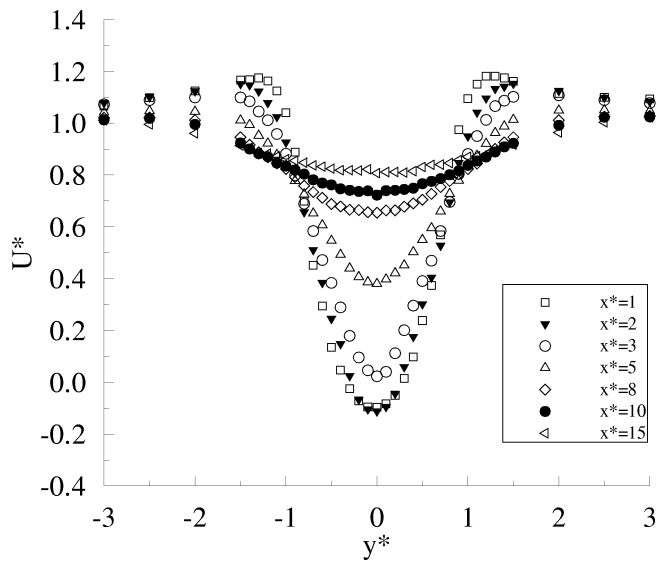

Figure 9. Mean longitudinal velocities in the cylinder wake. $Re - Re_c = 10,\ x^* = 1, 2, 3, 5, 8, 10$ and 15.

The velocity distributions of the transverse component are presented in *figure 10* for $Re - Re_c = 10$. They are always antisymmetrical about the center line. The sign of the velocity gradient $\partial V^*/\partial y^*$ close to the center line is in agreement with the opposite sign of the velocity gradient $\partial U^*/\partial x^*$ on the center line as found in *figure 9*.

In order to compare in a quantitative manner and concisely the longitudinal evolution of the whole velocity profiles some characteristics have been particularly studied. These characteristics are the center line velocity U^*_{cl} and the mean length of the recirculation zone s^*.

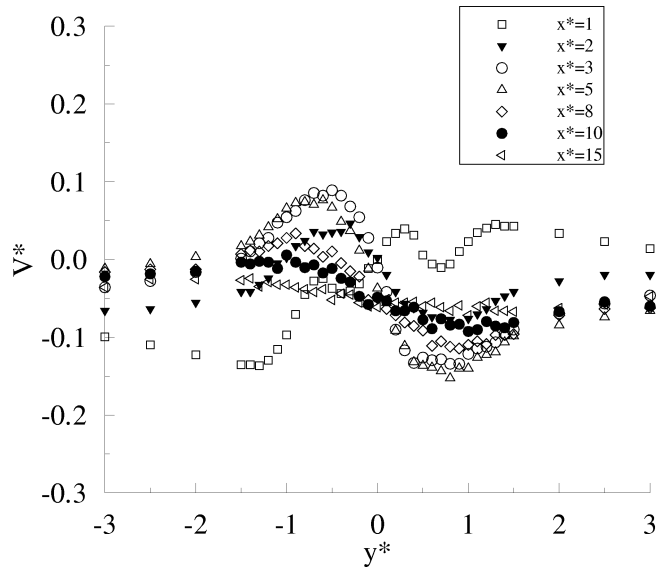

Figure 10. Mean transverse velocities in the cylinder wake. $Re - Re_c = 10$, $x^* = 1, 2, 3, 5, 8, 10$ and 15.

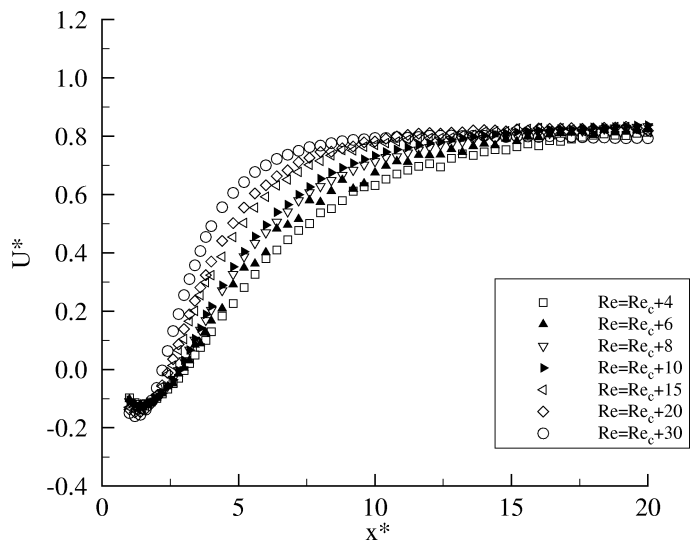

Figure 11. Streamwise evolution of the mean centerline longitudinal velocity in the cylinder wake.

The longitudinal evolution of the non-dimensional center line velocity is plotted in *figure 11*. In this figure it is possible to note more clearly the existence of the recirculation zone and the higher increase of U_{cl}^* as the Reynolds number increases above Re_c. The mean length s^* of the recirculation zone deduced from the above results is plotted against the Reynolds number in *figure 12*, comparing with data from Nishioka and Sato [33], Taneda [34], Socolescu et al. [35]. It appears from these results that the maximum value of this mean length is found when the flow bifurcates at Re_c. These results are compared to results obtained by several authors in the case of the circular cylinder.

The distributions of the isolines of constant rms values of the longitudinal and transverse velocities are plotted in a nondimensional form σ_u^* and σ_v^* as a function of (x^*, y^*) in *figures 13* and *14* for $Re - Re_c = 10$.

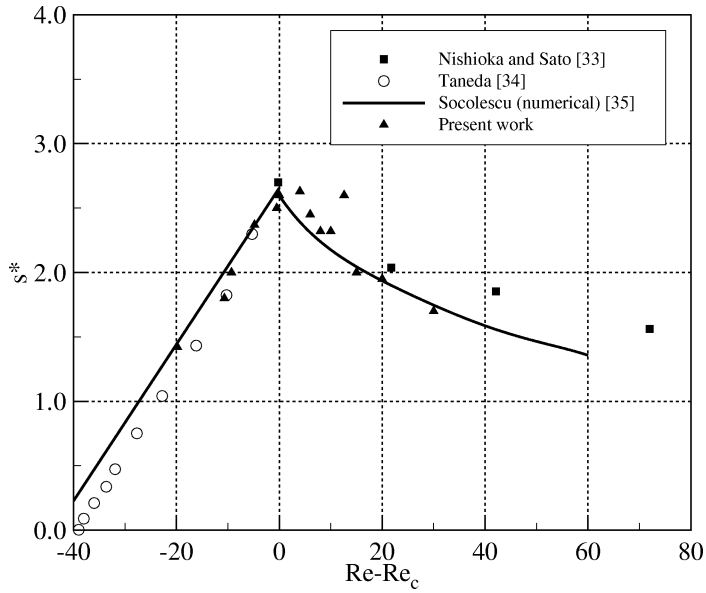

Figure 12. Mean length of recirculation in the cylinder wake versus Reynolds number.

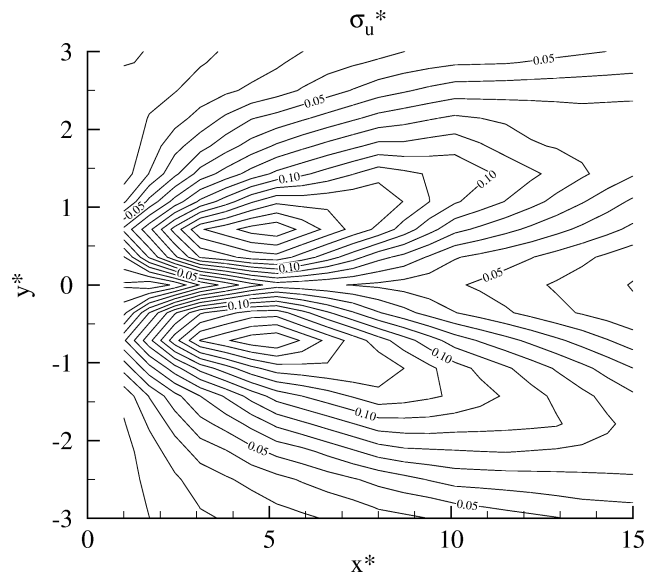

Figure 13. Isolines of constant rms levels of longitudinal velocities in the cylinder wake. $Re - Re_c = 10$.

These profiles are always symmetrical about the center line. The σ_u^* profiles always present two maxima located approximately where $\partial U^*/\partial y^*$ is maximum, while the σ_v^* profiles have a single maximum located on the center line. The maxima of the σ_u^* profiles move from about $y^* = \pm 0.7$ when $x^* = 1$ up to $y^* = \pm 1.5$ when $x^* = 15$. On the edges of the wake the u' and v' fluctuations have about the same values.

On the other hand the center line evolution of σ_v^* for this Reynolds number is similar to that measured in both cases. As presented in *figure 15* the intensity increases in the near-wake before reaching a maximum, approximately steady value. Further downstream the intensity decreases. $\sigma_{v,\max}^*$ is the maximum value of the

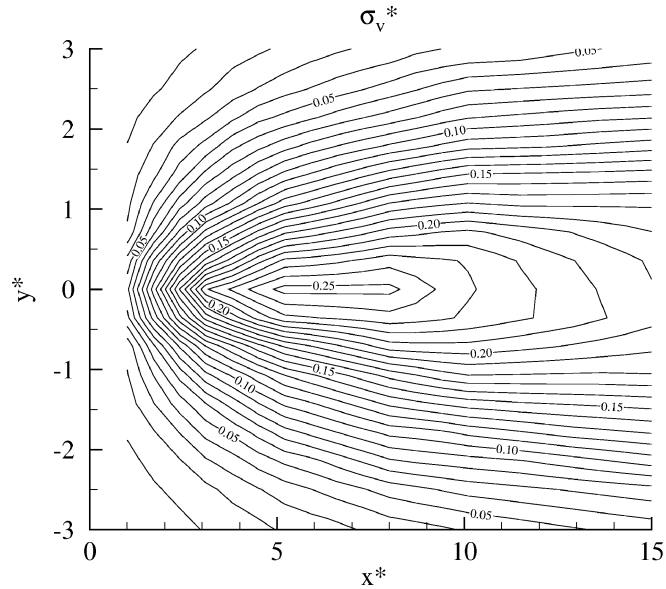

Figure 14. Isolines of constant rms levels of transverse velocities in the cylinder wake. $Re - Re_c = 10$.

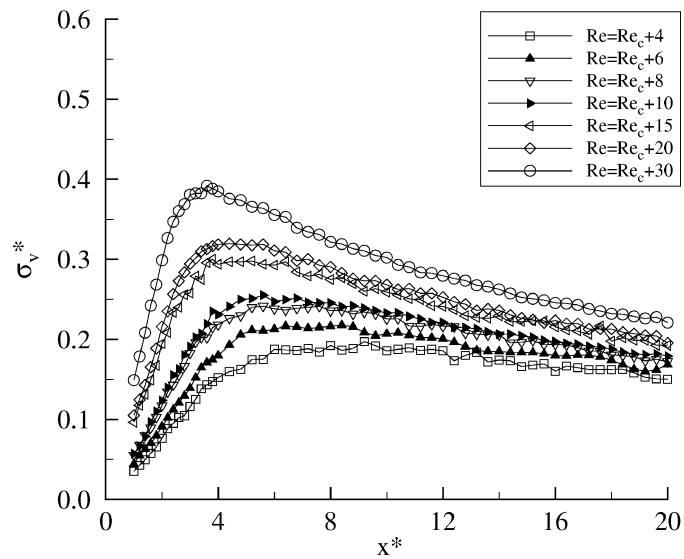

Figure 15. Streamwise evolution of the centreline rms values of transverse velocities in the cylinder wake.

rms transverse velocities on the centreline. This maximum value is located at $x^*_{\max}$. When the Reynolds number increases it appears that $\sigma^*_{\max}$ increases while $x^*_{\max}$ decreases.

As shown in *figure 16* the maximum value $\sigma^*_{v,\max}$ is found to increase with the threshold difference $\Delta Re = Re - Re_c$ with the exponent 0.34, while $x^*_{\max}$ decreases with the exponent -0.4. The maximum amplitude $\sigma_{v,\max}$, not plotted here, increases with the exponent 0.5.

The Reynolds stresses have been measured in the wake of the cylinder. For an example *figure 17* shows the profiles of $\overline{u'^* v'^*}$ at $Re - Re_c = 10$. The distribution of $\overline{u'^* v'^*}$ has always the opposite sign as that of $\partial U^*/\partial y^*$

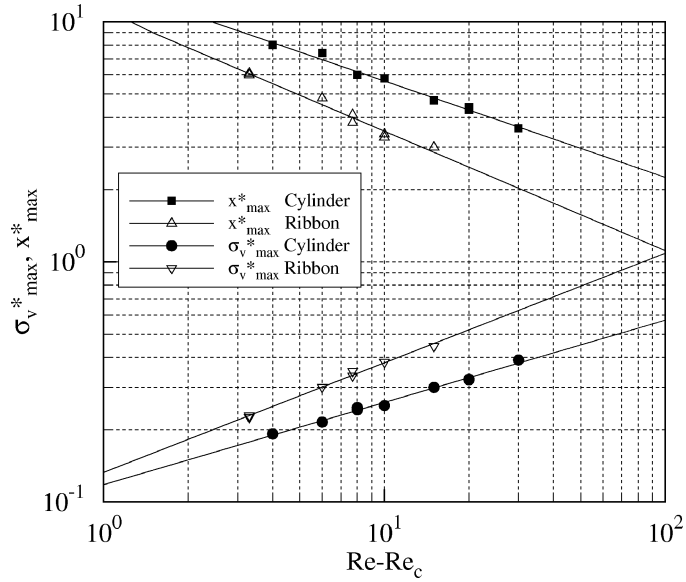

Figure 16. Evolution of $x^*_{v,\max}$ and $\sigma_{v,\max}$ as a function of the Reynolds number.

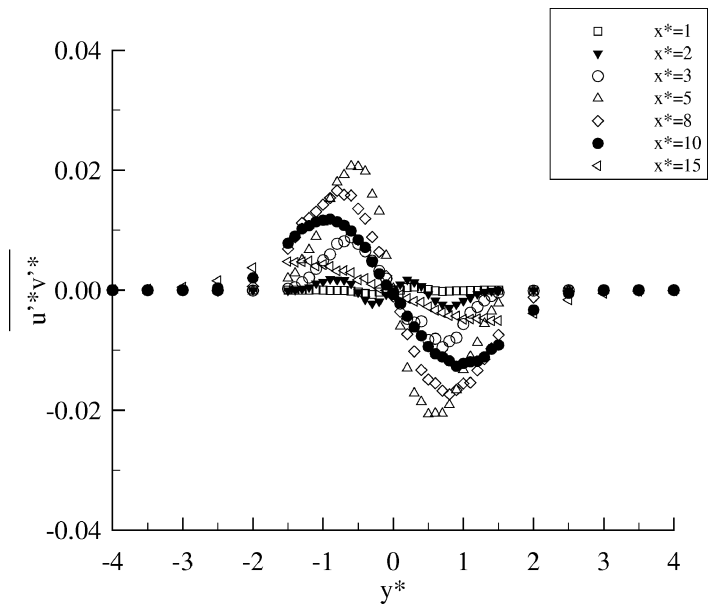

Figure 17. Reynolds stresses in the cylinder wake. $Re - Re_c = 10$.

except in the mean recirculation zone ($x^* < 3,\ |y^*| < 0.8$). It appears that the maximum value of $\overline{u'^*v'^*}$ is located about at $x^*_{\max}$.

Experimental results for the ribbon are similar to the ones measured downstream of the circular cylinder. For an example, as shown in *figure 16* the maximum value $\sigma^*_{v,\max}$ is found to increase with the threshold difference $\Delta Re = Re - Re_c$ with the exponent 0.46, while $x^*_{\max}$ decreases with the exponent -0.5. The maximum amplitude $\sigma_{v,\max}$, is found to increase with the exponent 0.5.

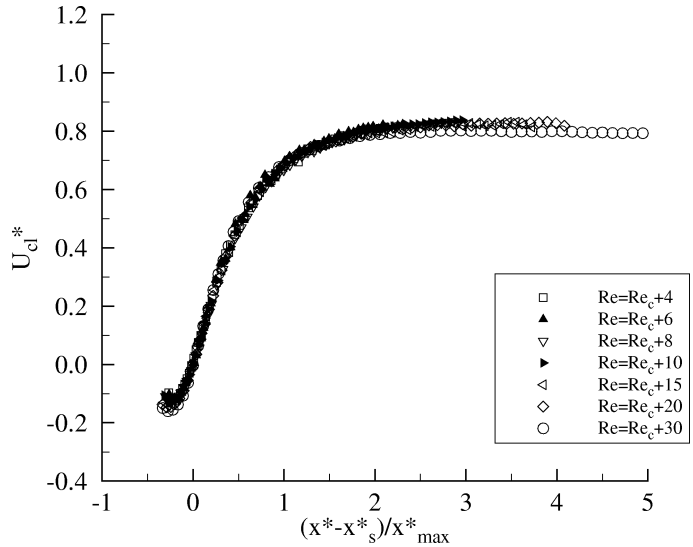

Figure 18. Dimensionless evolution of the mean centerline velocity in the cylinder wake.

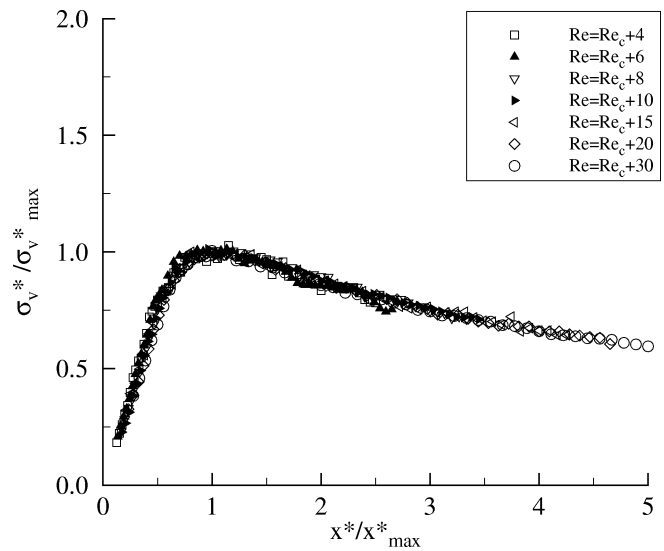

Figure 19. Dimensionless evolution of the centreline rms values of transverse velocities in the cylinder wake.

The values of the exponents found both for the cylinder and the ribbon for $x^*_{\max}$ and $\sigma_{v,\max}$ are in agreement with the values predicted by Landau theory, Provansal et al. [19].

As proposed by Goujon-Durand et al. [20] the values of $x^*_{\max}$ and $\sigma^*_{v,\max}$ can be used to present the longitudinal evolution of σ^*_v on the center line in a dimensionless form. These measurements, presented in *figure 19*, show that the results collapse on a single curve for the cylinder. The longitudinal evolution of U^*_{cl} can be also plotted in a dimensionless form in *figure 18* by using $(x^* - x^*_s)/x^*_{\max}$. Here we need to use an origin at $x^*_s = s^* + 0.5$, the location of the end of the mean recirculation zone to collapse the results. The same results where obtained for the ribbon.

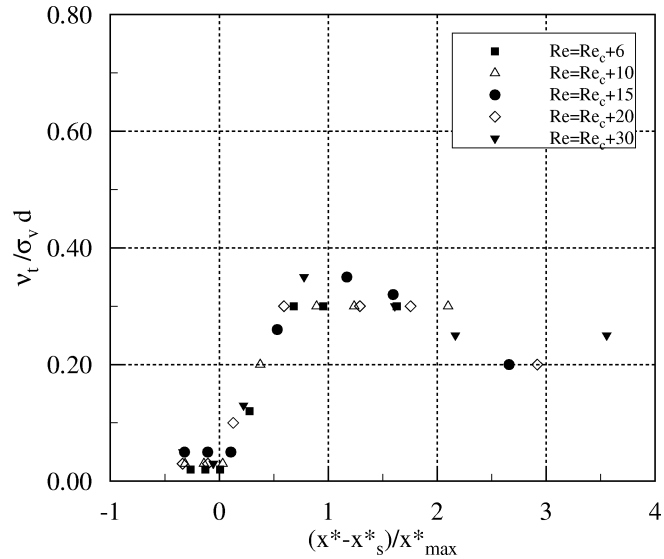

Figure 20. Dimensionless evolution of the eddy viscosity in the cylinder wake.

From the measurements of $\overline{u'^* v'^*}$ and $\partial U^*/\partial y^*$ it is possible to deduce an eddy viscosity ν_T defined by

$$\nu_T = -\frac{\overline{u'v'}}{\partial U/\partial y}. \tag{1}$$

This viscosity can be put in a dimensionless form by using the local value of σ_v and the cylinder diameter d. It appears that the mean value of $\nu_T/\sigma_v d$ is also a function of $(x^* - x_s^*)/x_{\max}^*$ as shown in *figure 20*. Over this low Reynolds numbers range ($Re_c + 6 < Re < Re_c + 30$), the laminar viscosity can represent 40–15% of this global viscosity ν_T.

5. Discussion

These extensive measurements of velocity downstream of a circular cylinder or a ribbon show the strong influence of the Reynolds number on the velocity field in the near 2-D periodic wake. The analysis of Abernathy and Kronauer [6] has shown that the shedding vortex street phenomenon could result from the dynamic interaction between two vortex sheets. In order to characterize this interaction, in our case, we have measured some characteristics of the mean velocity profile at the end of the mean recirculation zone for each experiment. As shown in *figure 21* these characteristics are the maximum velocity gradient $(\partial U^*/\partial y^*)_{\max}$, the shear layer thickness δ^* and the shear layer spacing Δ^*. The evolutions of these quantities with the Reynolds number are presented in *figure 22*. The shear layer thickness δ^* and the shear layer spacing Δ^* are found to decrease with the threshold difference $\Delta Re = Re - Re_c$, while the maximum velocity gradient $(\partial U^*/\partial y^*)_{\max}$ is found to increase.

In order to quantify the interaction we have calculated for each experiment an interaction term at the end of the recirculation zone as the ratio between the rate of circulation in the shear layer $|\mathrm{d}\Gamma/\mathrm{d}t|$ and the shear layer spacing Δ^*. Taking into account the small variations of the mean transverse velocity V^* in our experiment, $|\mathrm{d}\Gamma/\mathrm{d}t|$ can be deduced from the characteristics of the mean longitudinal velocity, as calculated by Fage and Johansen [36,37].

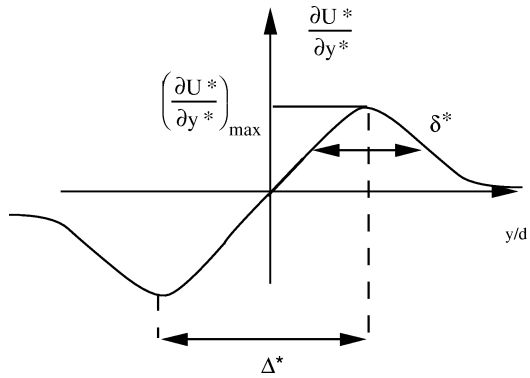

Figure 21. Definitions of Δ^*, δ^* and $\partial U^*/\partial y^*_{\max}$.

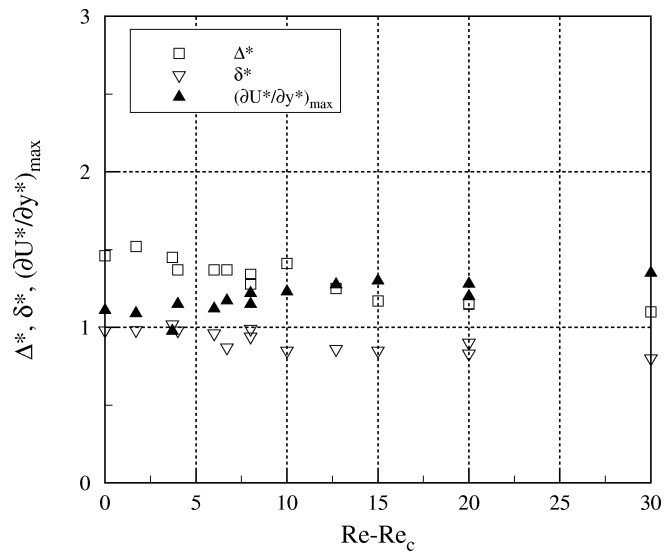

Figure 22. Values of the shear layer thickness, the shear layer spacing and the maximum mean velocity gradient at the end of the recirculation zone.

For the sake of simplicity this interaction term I was estimated as

$$I = \frac{|\mathrm{d}\Gamma/\mathrm{d}t|}{\Delta} = \frac{(\partial U/\partial y)_{\max}}{\Delta}\,\delta U(\Delta/2) \tag{2}$$

and has been calculated for several flow conditions. In order to compare the results obtained with the cylinder and the ribbon the interaction term has been normalized by using the frequency of the vortex shedding f and the velocity $U(\Delta/2)$ at the end of the recirculation section determined at the critical Reynolds number. This normalized interaction term I_{adim} is presented as a function of $Re - Re_c$ in *figure 23*. From this figure the results obtained from cylinder and ribbon experiments agree reasonably well and the value of this normalized interaction term is about 5.5 at Re_c. The value of this interaction term increases with increasing Reynolds number. This interaction term is based on mean time averaging of velocity measurements. Instantaneous values of this term, deduced from instantaneous velocity measurements, could lead to higher values when the Reynolds number is larger than the critical Reynolds number. However, at and close to Re_c this term is representative of the instantaneous interaction.

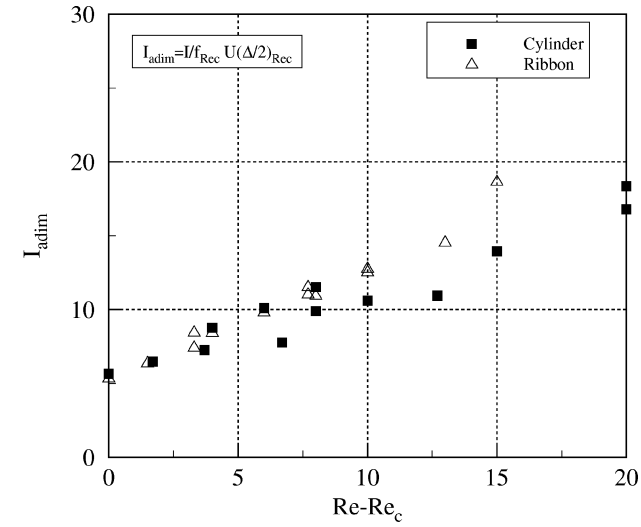

Figure 23. Variation of the normalized interaction term with $Re - Re_c$; circular cylinder and ribbon cases.

The physical mechanism of the control of the instability that we have described is close to the one described by Gerrard [38]. As recalled by Strykowski and Sreenivasan [31], "... the model of Gerrard predicts that the circulation in the shear layer must be of a sufficient magnitude before one shear layer draws the other across the wake centre plane. This interaction must happen before a critical length, called the formation length, is reached". In our case this critical length is the length of the recirculation zone s^* and the value of the interaction term I_{adim}, linked to the characteristics of the local velocity field, controls the development of the instability. This critical length s^* is always lower than the length considered by Gerrard [38] which corresponds approximately to $x^*_{\max}$.

6. Conclusion

An experimental study has been made of the near wake of two two-dimensional bluff bodies, a circular cylinder and a flat ribbon in the regimes corresponding to the 2-D steady and 2-D periodic wake. Comparisons of velocity measurements from both hot-wire and laser Doppler anemometry show that, over this Reynolds numbers range, hot-wire measurements are not accurate in the near wake. Extensive velocity measurements of the near wake of the circular cylinder and flat ribbon have shown that the location $x^*_{\max}$ and the maximum value $\sigma^*_{v,\max}$ of the rms transverse velocity fluctuation on the center line can be used to plot in a universal form the evolution of the rms transverse velocity fluctuations on the center line whatever the value of the Reynolds number. The longitudinal evolution of U^*_{cl} and the averaged vortex viscosity $\nu_t/\sigma_v d$ can be also plotted in a dimensionless form by using the length scale $(x^* - x^*_s)/x^*_{\max}$ where x^*_s is the location of the end of the mean recirculation zone on the center line. These measurements show that the onset of the instability can be linked to a critical value of an interaction term related to the strength of the shear layers and the shear layer spacing at the end of the recirculation zone.

References

[1] Bénard H., Formation de centres de giration à l'arrière d'un obstacle en mouvement, C. R. Acad. Sci. Paris 147 (1908) 839–842.
[2] von Karman T., Über den mechanismus des widerstandes den ein bewegter körper in einer flüssigkeit erfährt, Gott. Nachr. (1911) 509–517.

[3] Kovasznay L.S.G., Hot wire investigation of the wake behind a cylinder at low Reynolds numbers, Proc. Roy. Soc. A 198 (1949) 174–190.
[4] Roshko A., On the development of turbulent wakes from vortex streets, NACA Report 1191, 1953.
[5] Roshko A., On the drag and shedding frequency of two dimensional bluff bodies, NACA TN 3169, 1954.
[6] Abernathy F.H., Kronauer R.E., The formation of vortex street, J. Fluid Mech. 13 (1962) 1–20.
[7] Bearman P.W., On vortex street wakes, J. Fluid Mech. 28 (1967) 625–641.
[8] Gerich D., Eckelmann H., Influence of end plates and free ends on the shedding frequency of circular cylinders, J. Fluid Mech. 122 (1982) 109–121.
[9] Van Atta C.W., Gharib M., Ordered and chaotic vortex streets behind circular cylinder at low Reynolds numbers, J. Fluid Mech. 174 (1987) 113–133.
[10] Williamson C.H.K., Oblique and parallel modes of vortex shedding in the wake of a circular cylinder at low Reynolds numbers, J. Fluid Mech. 206 (1989) 579–627.
[11] Williamson C.H.K., Vortex dynamics in the wake of a cylinder, in: Fluid Mechanics and Its Application, Vol. 30, Kluwer, Dordrecht, 1995, pp. 155–221.
[12] König M., Eisenlohr H., Eckelmann H., The fine structure in the Strouhal–Reynolds relationship of the laminar wake of a circular cylinder, Phys. Fluid A 2 (9) (1990).
[13] Koch W., Local instability characteristics and frequency determination of self excited wake flows, J. Sound Vib. 99 (1985) 53–83.
[14] Triantafyllou G., Triantafyllou M., Chryssostomidis C., On the formation of vortex streets behind stationary cylinders, J. Fluid Mech. 170 (1986) 461–477.
[15] Monkewitz P.A., The absolute and convective nature of instability in two dimensional wakes at low Reynolds numbers, Phys. Fluids 31 (1988) 999–1006.
[16] Yang X., Zebib A., Absolute and convective instability of a cylinder wake, Phys. Fluids A 1 (1989) 689–696.
[17] Huerre P., Monkewitz P.A., Local and global instabilities in spatially developing flows, Ann. Rev. Fluid Mech. 22 (1990) 473–537.
[18] Oertel H., Wakes behind blunt bodies, Ann. Rev. Fluid Mech. 22 (1990) 539–564.
[19] Provansal M., Mathis C., Boyer L., Bénard–von Karman instability, J. Fluid Mech. 182 (1987) 1–22.
[20] Goujon-Durand S., Jenffer P., Wesfreid J.E., Downstream evolution of the Bénard–von Karman instability, Phys. Rev. E 50 (1) (1994) 308–313.
[21] Dusek J., Le Gal P., Fraunié P., A numerical and theoretical study of the first Hopf bifurcation in a cylinder wake, J. Fluid Mech. 264 (1994) 59–80.
[22] Son J.S., Hanratty T.J., Numerical solution for the flow around a circular cylinder at Reynolds numbers of 40, 200 and 500, J. Fluid Mech. 35 (1969) 369–386.
[23] Persillon H., Braza M., Physical analysis of the transition to turbulence in the wake of a circular cylinder by three-dimensional Navier–Stokes simulation, J. Fluid Mech. (1998) (accepted for publication).
[24] Nishioka M., Sato H., Measurements of velocity distributions in the wake of a circular cylinder at low Reynolds numbers, J. Fluid Mech. 65 (1) (1974) 97–112.
[25] Le Masson S., Controle de l'instabilité de Bénard–von Karman en aval d'un obstacle chauffé à faible nombre de Reynolds, Thèse de doctorat de l'Université de Rouen, 1991.
[26] Paranthoën P., Browne L., Le Masson S., Lecordier J.C., Control of vortex shedding by thermal effect at low Reynolds number, Internal Report MT1, Rouen University, 1995.
[27] Mair W.A., Maull D.J., Bluff bodies and vortex shedding, a report of Euromech 17, J. Fluid Mech. 45 (1971) 209–224.
[28] Hammache M., Gharib M., A novel method to promote parallel vortex shedding in the wake of circular cylinders, Phys. Fluid A 1 (10) (1989) 1611–1614.
[29] Perry A.E., Hot-Wire Anemometry, Clarendon Press, Oxford, 1982.
[30] Bruun H.H., Hot-Wire Anemometry, Oxford Science Publications, Oxford, 1995.
[31] Strykowski P.J., Sreenivasan K.R., On the suppression of vortex shedding at low Reynolds numbers, J. Fluid Mech. 218 (1990) 71–107.
[32] Paranthoën P., Lecordier J.C., Control of the wake instability at low Reynolds numbers by thermal effect, in: Bluff-Body Wakes, Dynamics and Instabilities, Springer, Göttingen, 1993, pp. 245–248.
[33] Nishioka M., Sato H., Mechanism of determination of the shedding frequency of vortices behind a cylinder at low Reynolds numbers, J. Fluid Mech. 89 (1) (1978) 49–60.
[34] Taneda S., Experimental investigation of the wakes behind cylinders and plates at low Reynolds numbers, J. Phys. Soc. Jpn 11 (3) (1956) 302–307.
[35] Socolescu L., Mutabazi I., Daube O., Huberson S., Etude de l'instabilité du sillage bidimensionnel derrière un cylindre faiblement chauffé, C. R. Acad. Sci. Paris II B 322 (1996) 203–208.
[36] Fage A., Johansen F.C., On the flow of air behind an inclined flat plate of infinite span, Proc. Roy. Soc. A 116 (773) (1927) 170–197.
[37] Fage A., Johansen F.C., The structure of vortex sheets, Philos. Mag. Ser. 7 5 (28) (1928) 417–441.
[38] Gerrard J.H., The mechanics of the formation region of vortices behind bluff bodies, J. Fluid Mech. 25 (1966) 401–413.